SUPPLEMENTAL MATERIAL - TABLE OF CONTENTS

Figure S1

Laser-capture microdissection

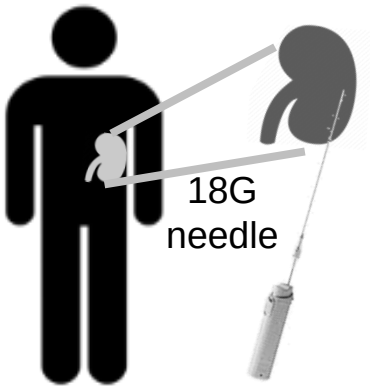

Formalin-Fixed Paraffin-Embedded kidney biopsy

AMR (n = 7)
ACR (n = 11)
ATN (n = 12)

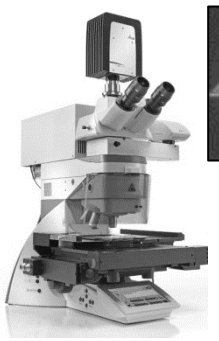

Leica DM 6000B

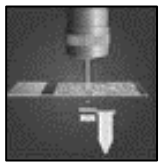

Tubulointerstitium

Glomeruli

Sample preparation

LC-MS/MS

Thermo Q-Exactive Plus

Maxquant Software

Protein identification and quantification

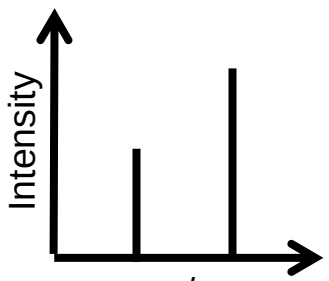

Perseus Software

Differentially expressed proteins

Gene ontology and pathway analysis

Systems biology

Pathway reduction algorithm

External validation in publicly available data

Protease prediction

Orthogonal verification (IHC, IF)

***In vitro* studies**

Figure S2

A

GLOMERULI

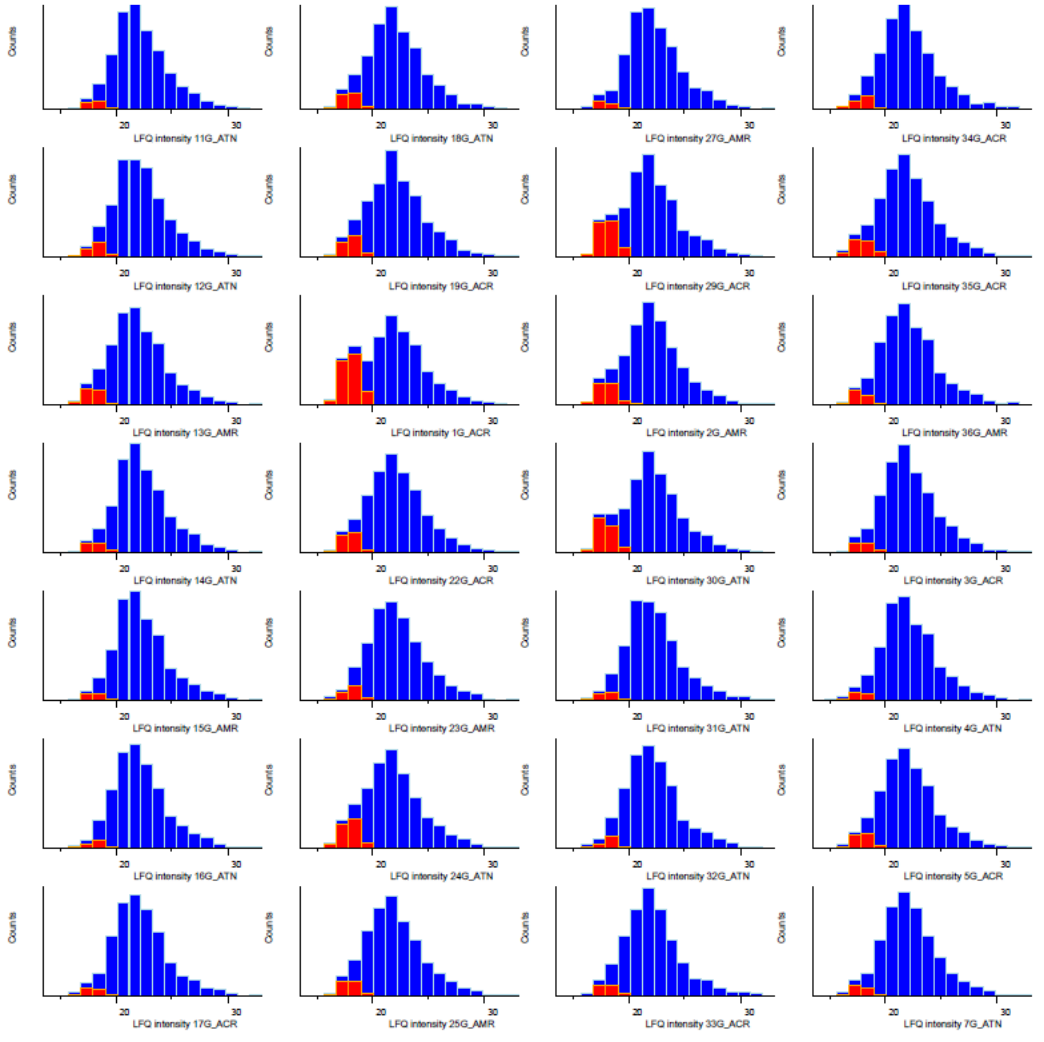

Excluded from further analyses:

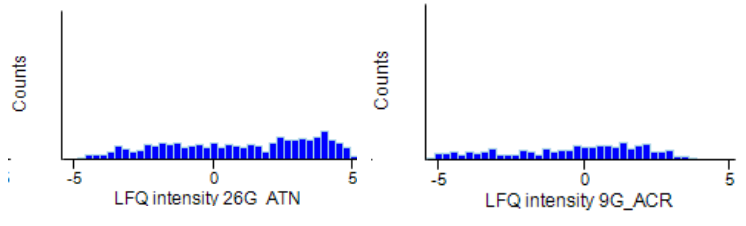

B

TUBULOINTERSTITIUM

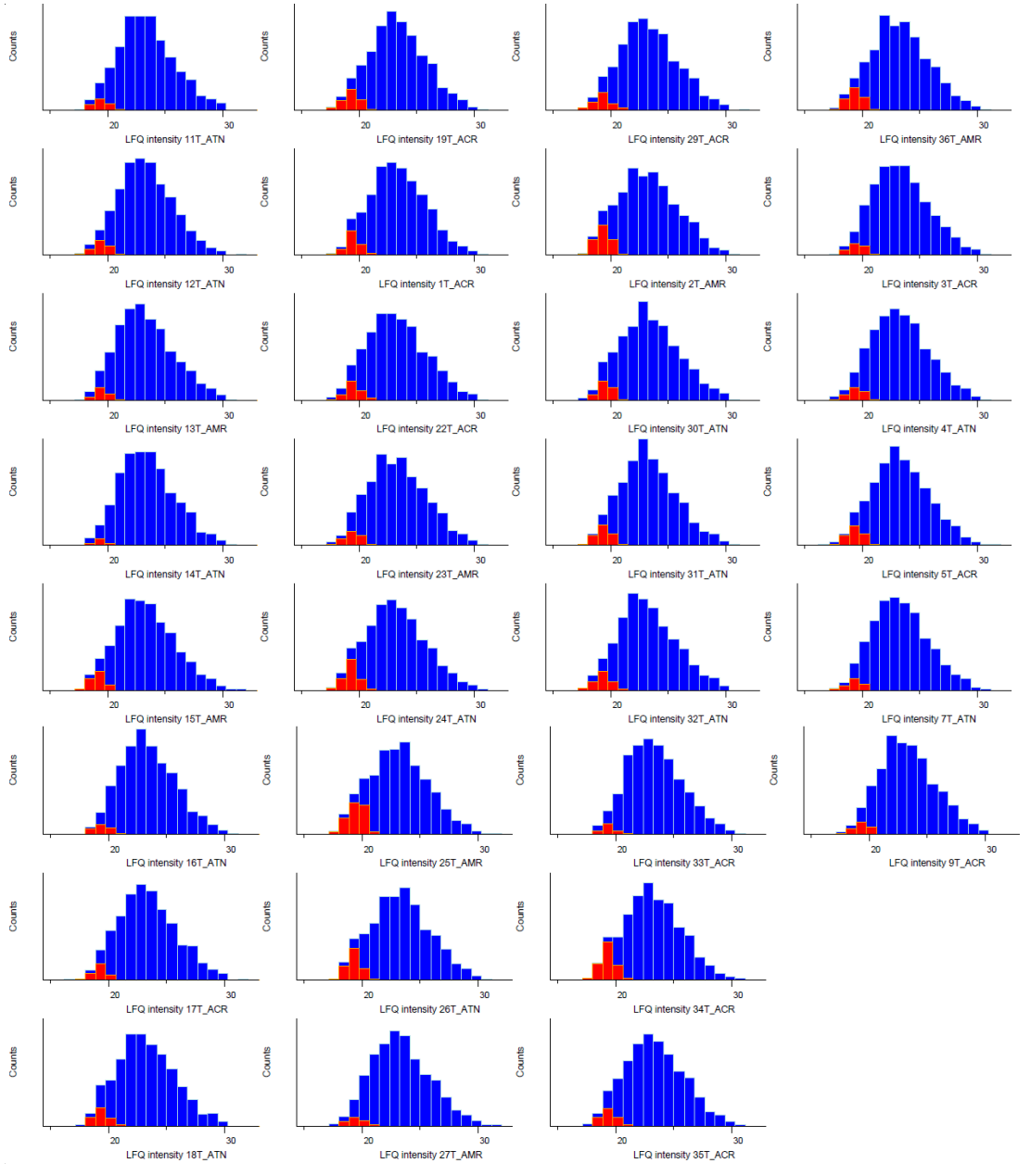

Figure S3

A

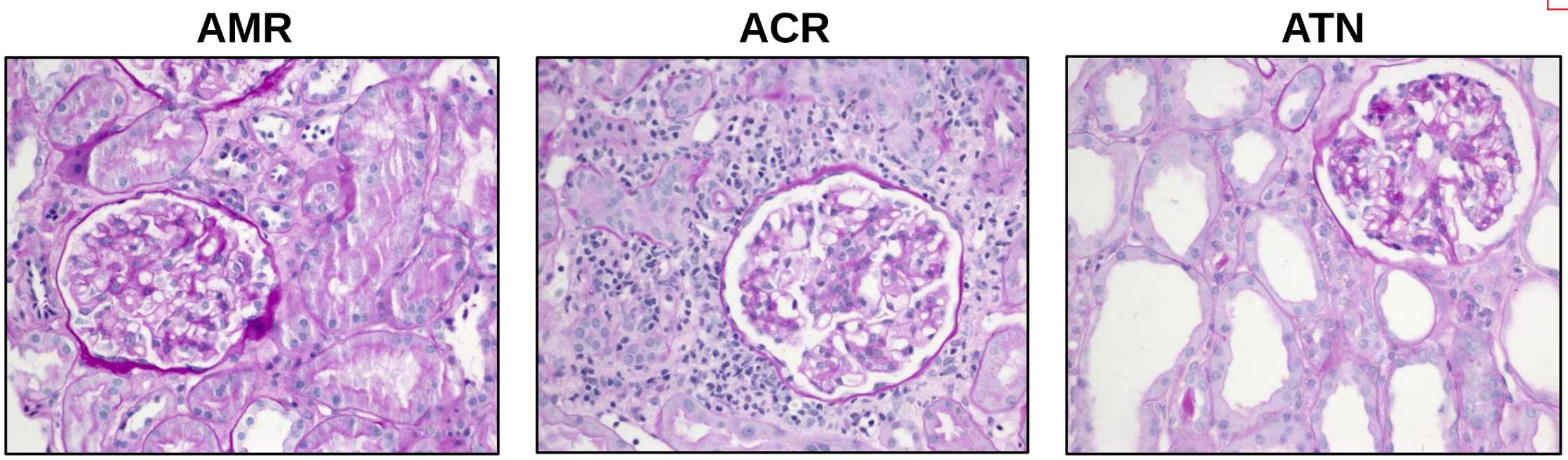

B

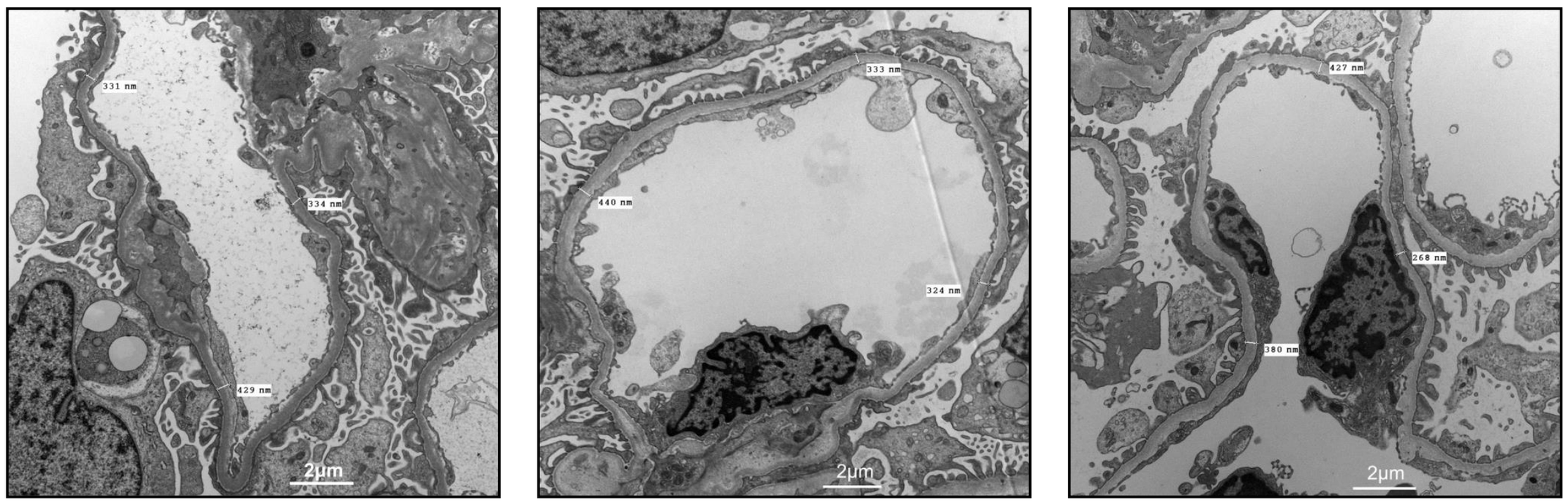

C

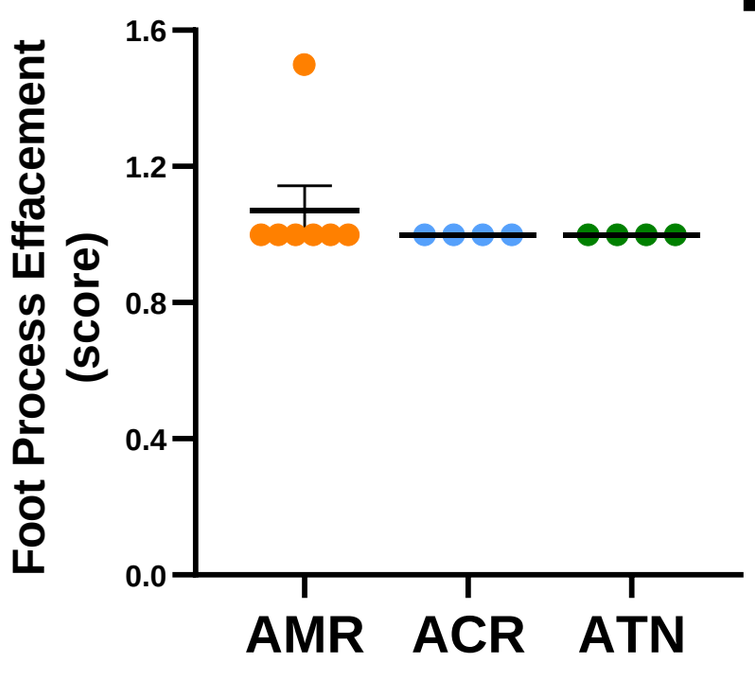

D

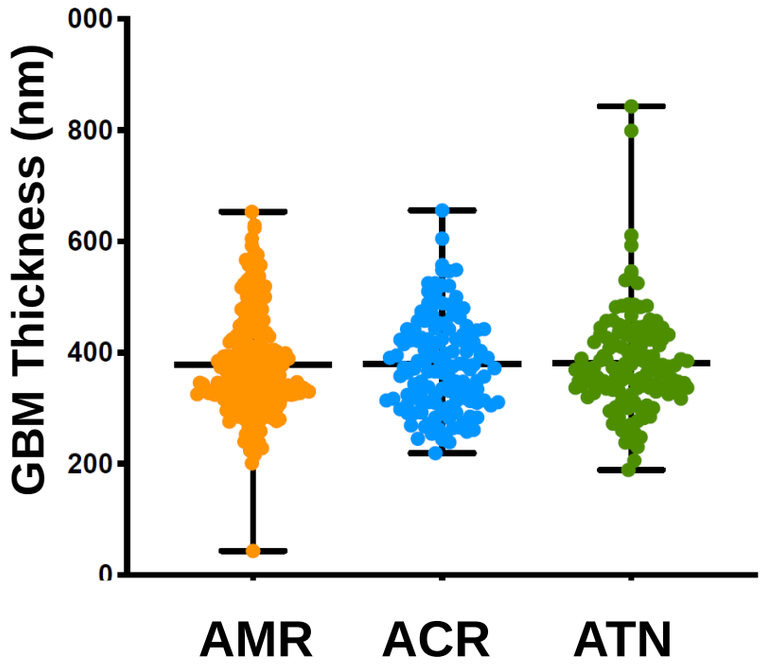

E

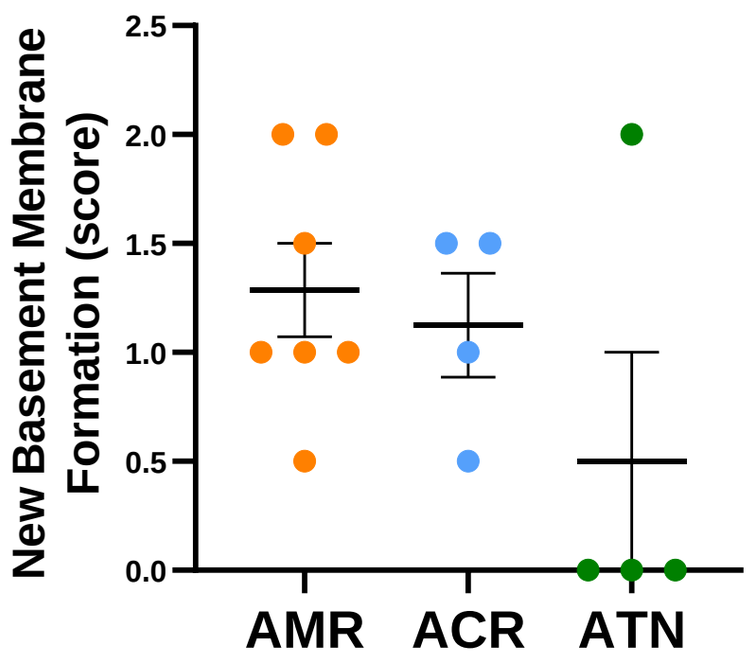

F

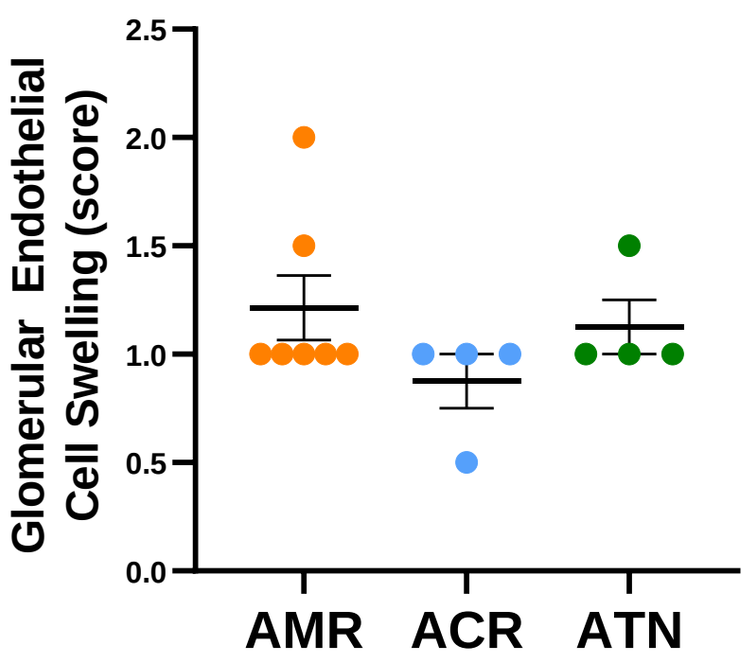

G

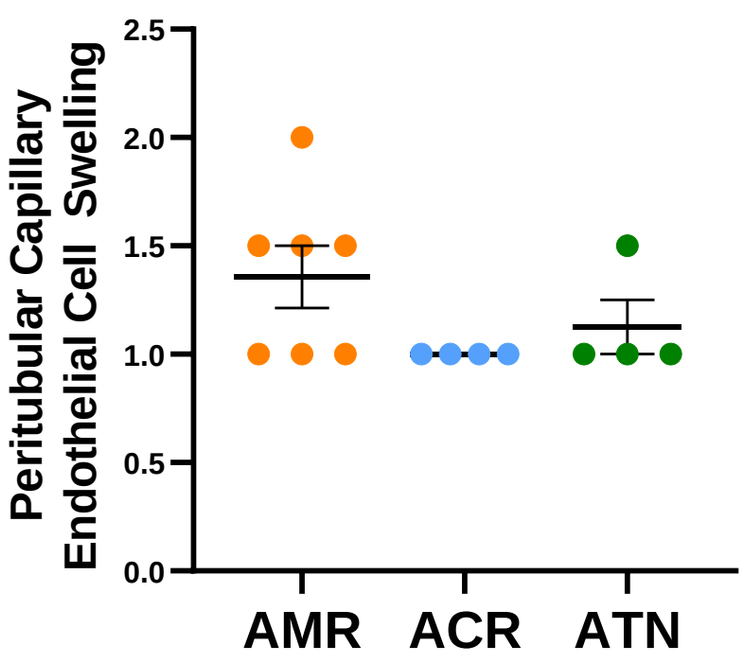

A

MEDIAN LOG2 (LFQ INTENSITY)	GLOM	TUBULOINT
COL1A1	17.65	28.92
COL1A2	20.05	29.82
COL3A1	0.00	26.08
COL4A1	28.15	27.86
COL4A2	28.02	28.26
COL4A3	26.88	0.00
COL4A4	26.55	0.00
COL4A5	21.72	0.00
COL5A1	0.00	24.21
COL5A2	0.00	21.17
COL6A1	26.79	25.93
COL6A2	27.17	25.86
COL6A2 - isof 2 and 3	21.19	0.00
COL6A3 - isof 4	21.53	21.37
COL6A3 - others	28.95	28.15
COL12A1	0.00	24.21
COL14A1	0.00	21.00
COL15A1	0.00	22.64
COL18A1	27.12	27.51

GBM Collagens

B

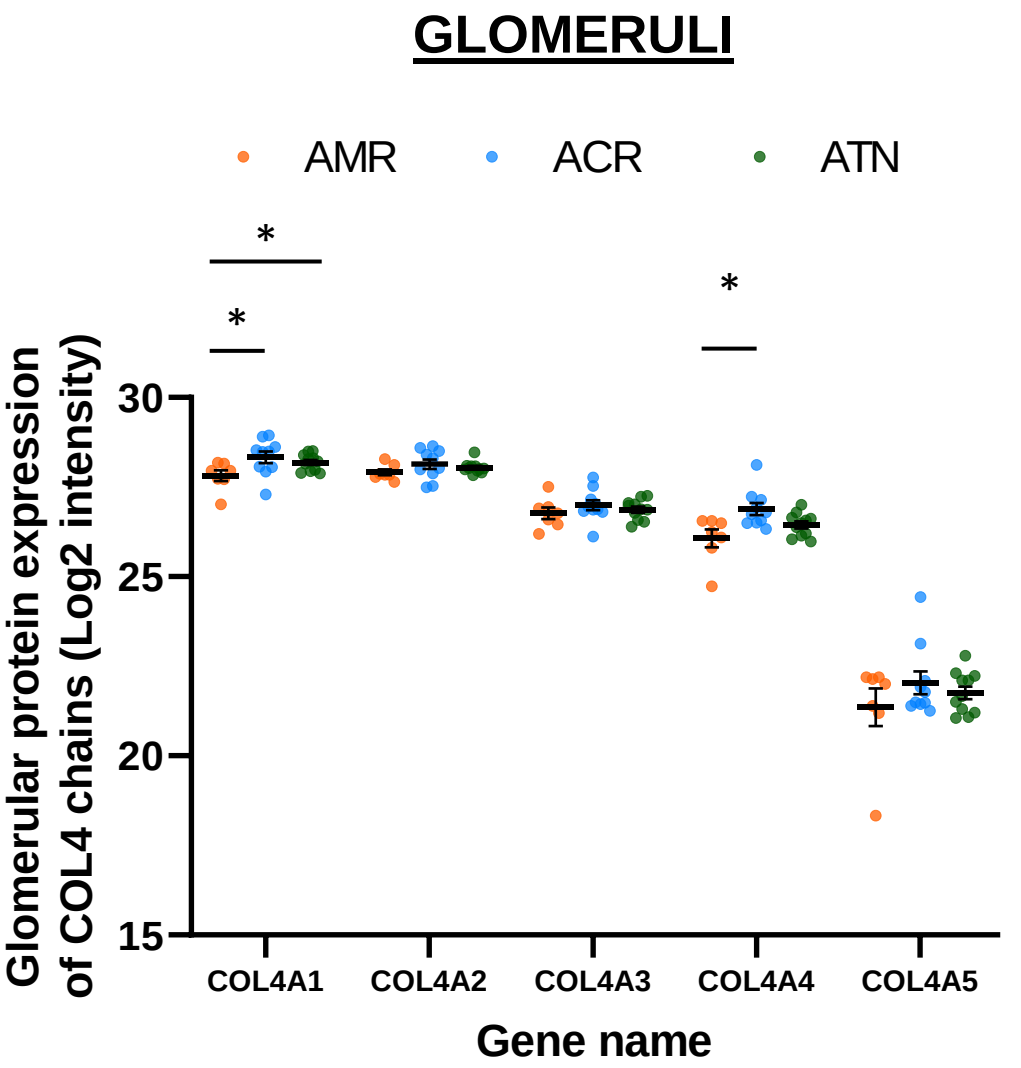

Figure S5

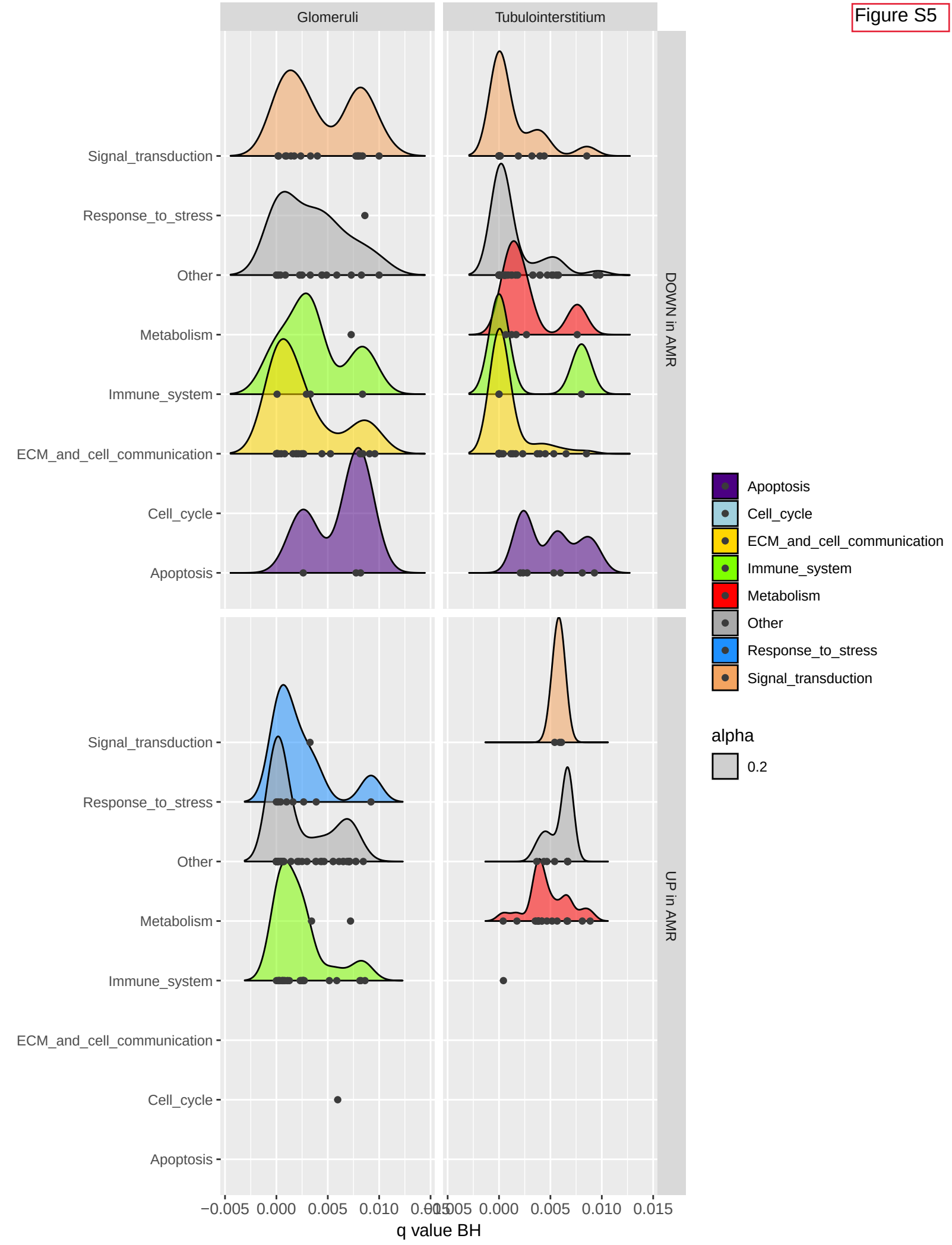
Glomeruli
Tubulointerstitium
DOWN in AMR
UP in AMR
Signal_transduction
Response_to_stress
Other
Metabolism
Immune_system
ECM_and_cell_communication
Cell_cycle
Apoptosis
−0.005
0.000
0.005
0.010
0.015
q value BH
Apoptosis
Cell_cycle
ECM_and_cell_communication
Immune_system
Metabolism
Other
Response_to_stress
Signal_transduction
alpha
0.2

A

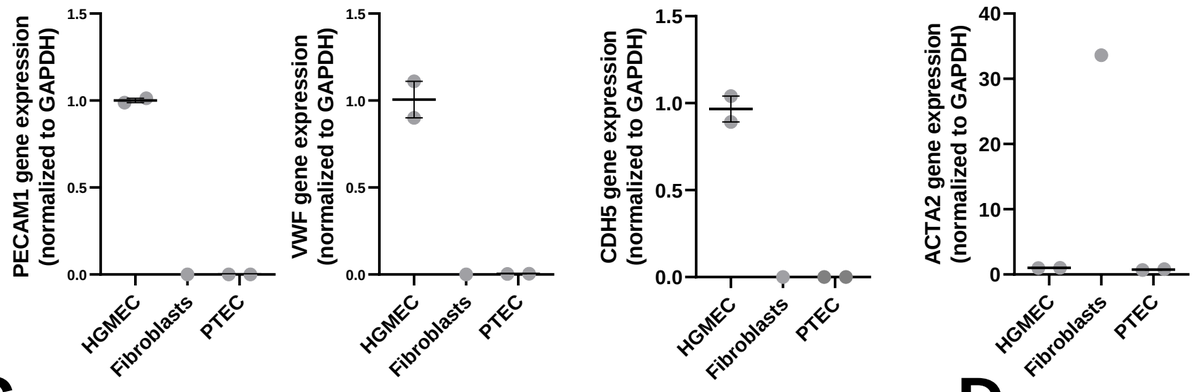
PECAM1 gene expression (normalized to GAPDH)
VWF gene expression (normalized to GAPDH)
CDH5 gene expression (normalized to GAPDH)
ACTA2 gene expression (normalized to GAPDH)
HGMEC
Fibroblasts
PTEC

B

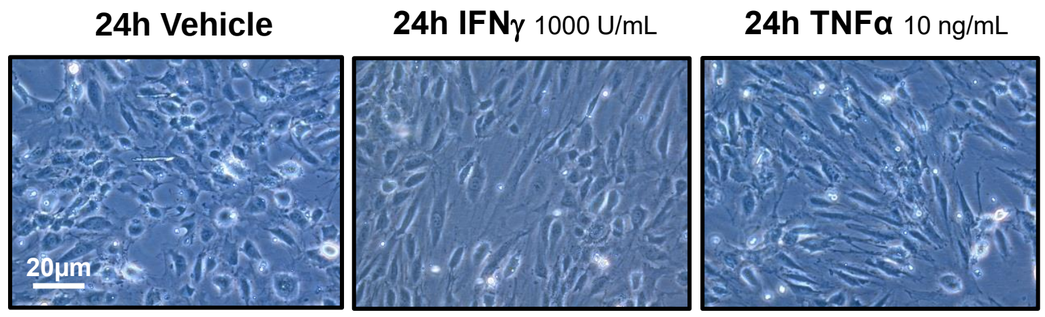
24h Vehicle
24h IFNγ 1000 U/mL
24h TNFα 10 ng/mL
20µm

C

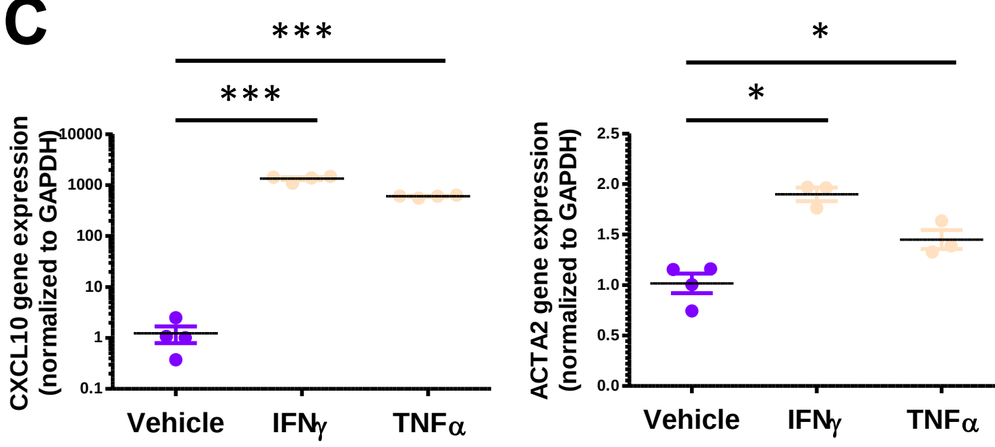
CXCL10 gene expression (normalized to GAPDH)
ACTA2 gene expression (normalized to GAPDH)
Vehicle
IFNγ
TNFα

D

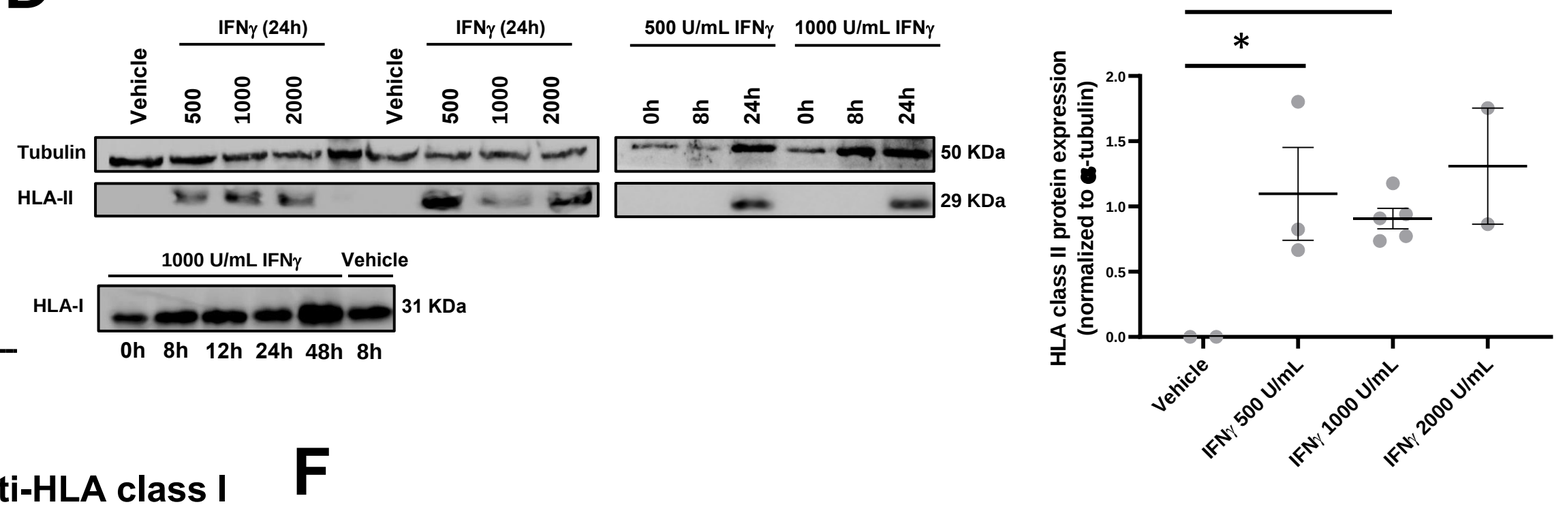
IFNγ (24h)
500 U/mL IFNγ
1000 U/mL IFNγ
Vehicle
Tubulin
HLA-II
HLA-I
50 KDa
29 KDa
31 KDa
HLA class II protein expression (normalized to α-tubulin)
Vehicle
IFNγ 500 U/mL
IFNγ 1000 U/mL
IFNγ 2000 U/mL

E

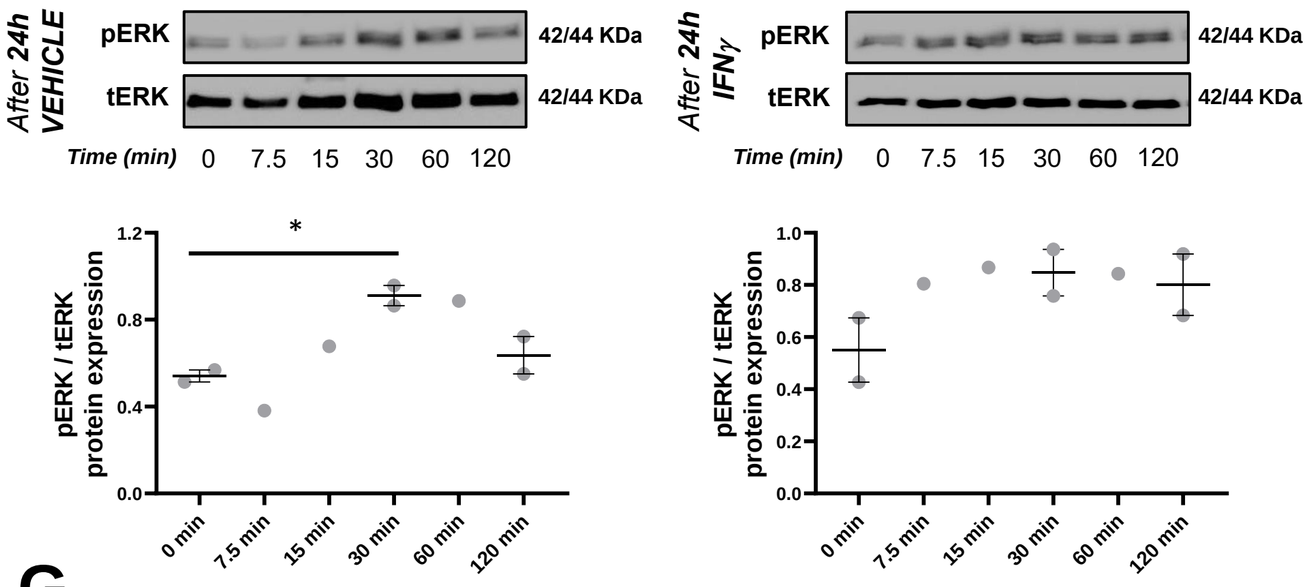
+1 µg/mL anti-HLA class I
After 24h VEHICLE
After 24h IFNγ
pERK
tERK
42/44 KDa
Time (min) 0 7.5 15 30 60 120
pERK / tERK protein expression
0 min
7.5 min
15 min
30 min
60 min
120 min

F

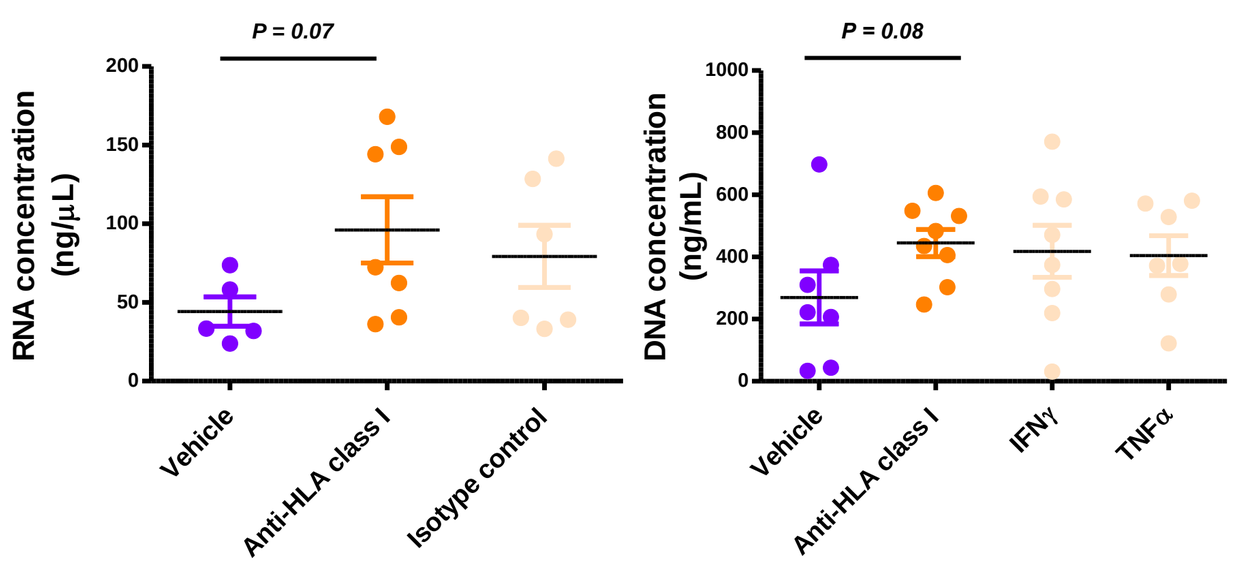
+1 µg/mL anti-HLA class I
P = 0.07
P = 0.08
RNA concentration (ng/µL)
DNA concentration (ng/mL)
Vehicle
Anti-HLA class I
Isotype control
IFNγ
TNFα

G

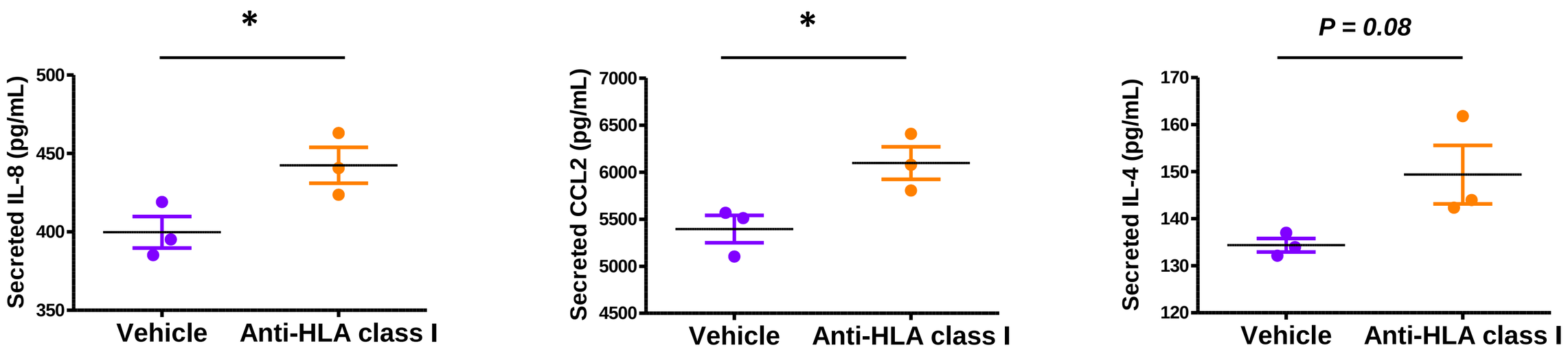
Secreted IL-8 (pg/mL)
Secreted CCL2 (pg/mL)
Secreted IL-4 (pg/mL)
P = 0.08
Vehicle
Anti-HLA class I

H

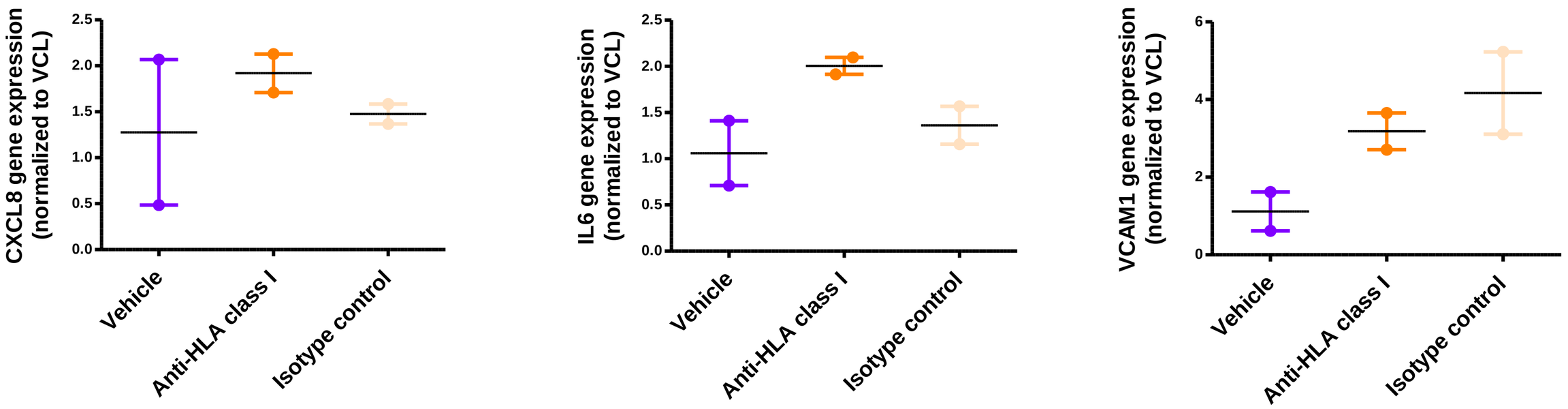
CXCL8 gene expression (normalized to VCL)
IL6 gene expression (normalized to VCL)
VCAM1 gene expression (normalized to VCL)
Vehicle
Anti-HLA class I
Isotype control

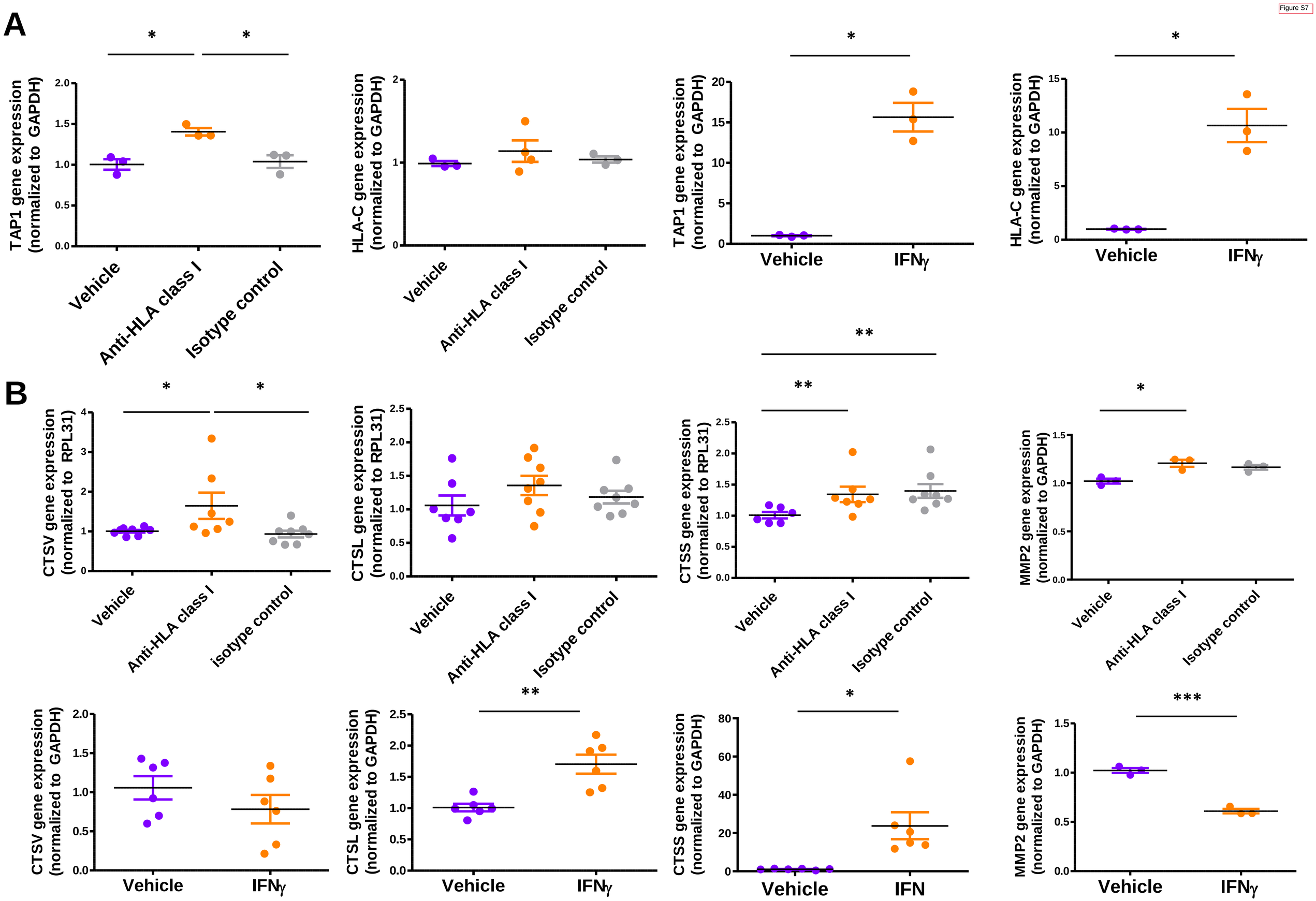
A
TAP1 gene expression (normalized to GAPDH)
HLA-C gene expression (normalized to GAPDH)
Vehicle
Anti-HLA class I
Isotype control
IFNγ
B
CTSV gene expression (normalized to RPL31)
CTSL gene expression (normalized to RPL31)
CTSS gene expression (normalized to RPL31)
MMP2 gene expression (normalized to GAPDH)
CTSV gene expression (normalized to GAPDH)
CTSL gene expression (normalized to GAPDH)
CTSS gene expression (normalized to GAPDH)
MMP2 gene expression (normalized to GAPDH)
isotype control
IFN
C
Vehicle
Anti-HLA class I
Isotype control
OLIGO
FCCP
2-DG
Rot/AA
ECAR (mpH / min)
OCR (pmol / min)
Time (min)
D
Superoxide ion levels (RFU)
P = 0.08
E
ATP concentration (nM)
P = 0.10
P = 0.07
IFNγ
TNFα

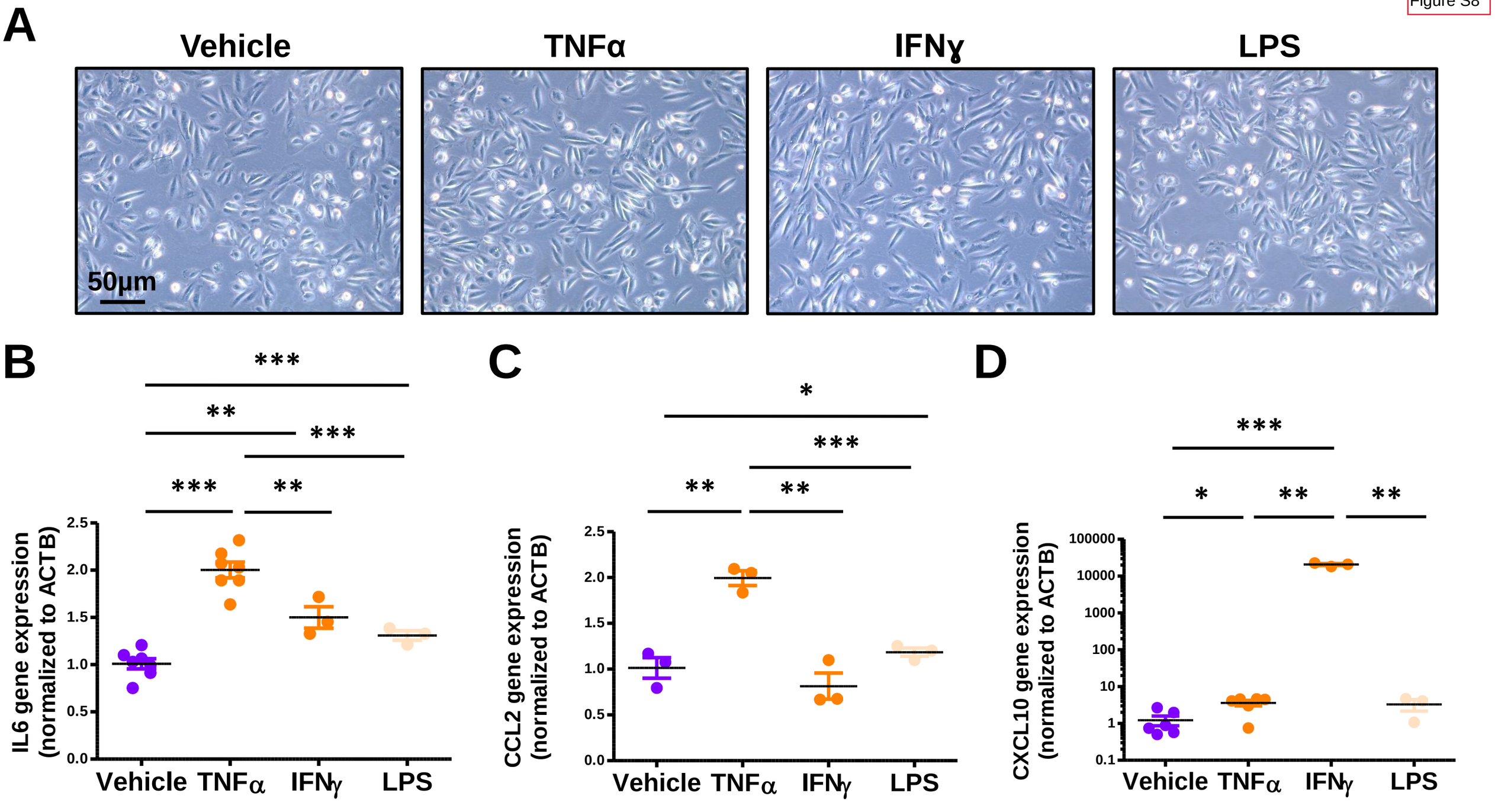
A
Vehicle
TNFα
IFNγ
LPS
50μm
B
IL6 gene expression (normalized to ACTB)
C
CCL2 gene expression (normalized to ACTB)
D
CXCL10 gene expression (normalized to ACTB)
Vehicle
TNFα
IFNγ
LPS

A

EXPERIMENT 1

SET A | SET B | SET C | SET D

Vehicle, IFNγ, TNFα, LPS, Tissue control, Vehicle, IFNγ, TNFα, LPS, Vehicle, IFNγ, TNFα, LPS, Vehicle, IFNγ, TNFα, LPS

GSTO1 ~28 KDa

GAPDH ~36 KDa

EXPERIMENT 2 | EXPERIMENT 3

SET A | SET B | SET A | SET B

Vehicle, TNFα, Vehicle, TNFα, Vehicle, TNFα, Vehicle, TNFα, Vehicle, TNFα, Vehicle, TNFα, Vehicle, TNFα, Vehicle, TNFα

GSTO1 ~28 KDa

GAPDH ~36 KDa

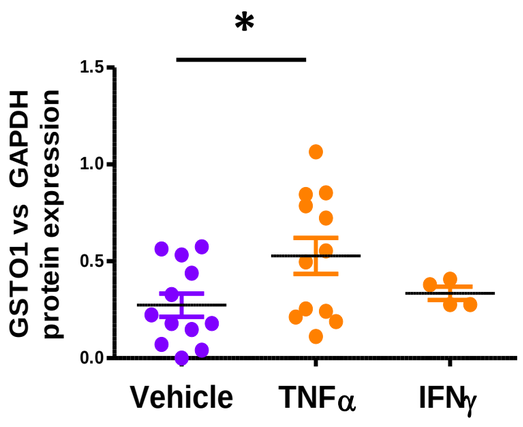

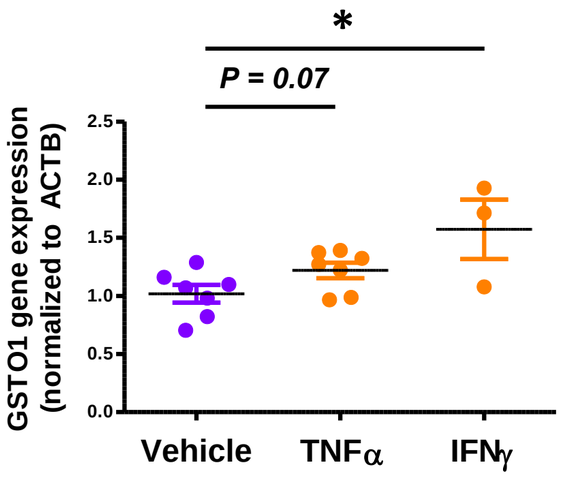

B

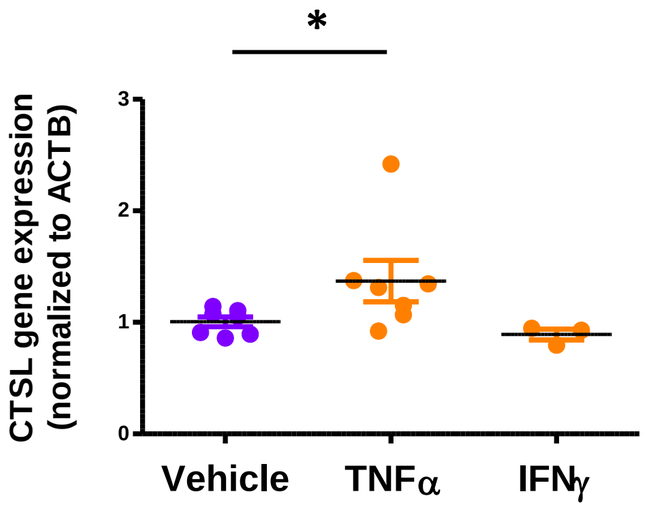

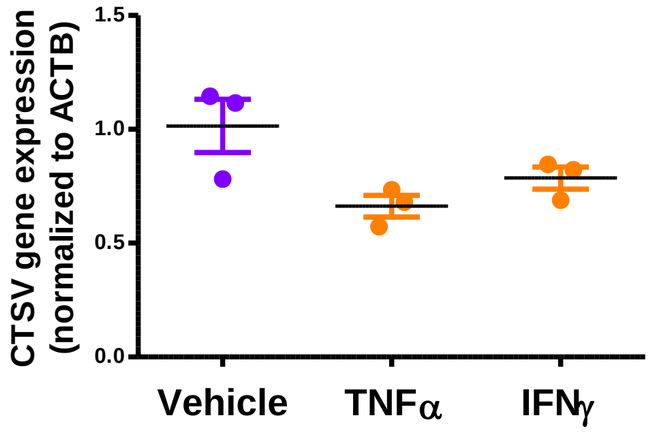

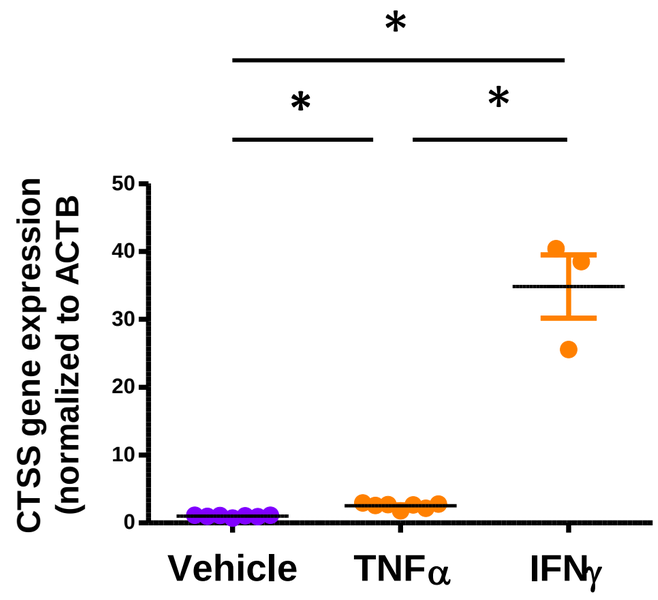

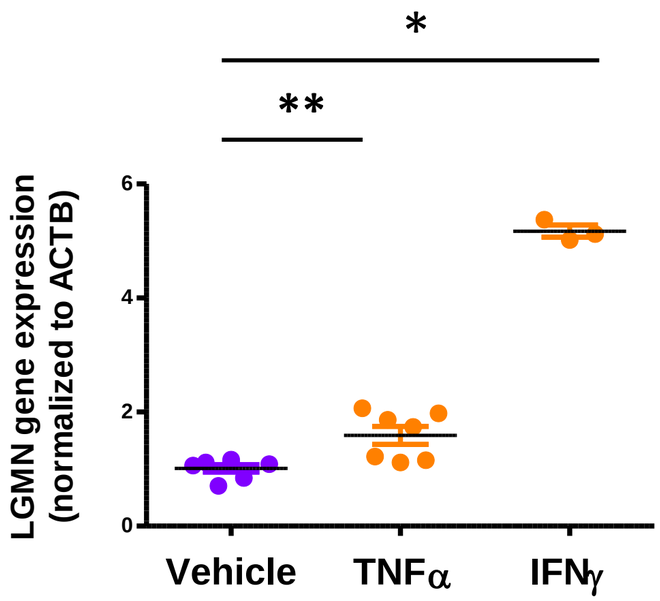

C

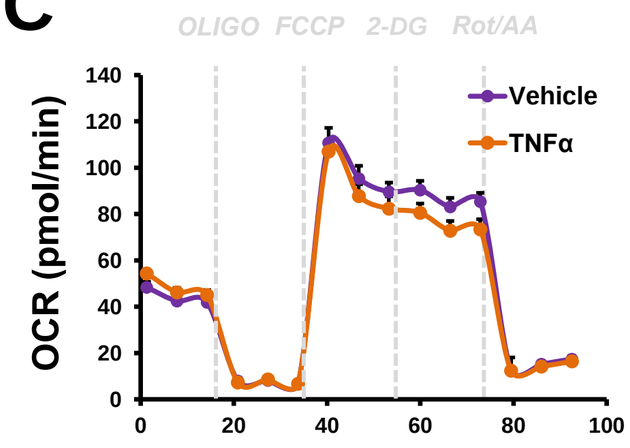

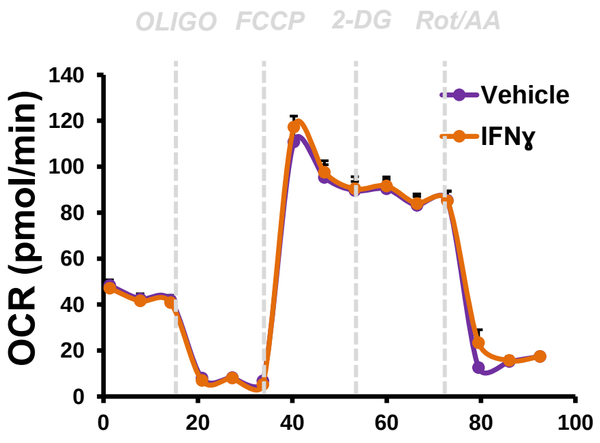

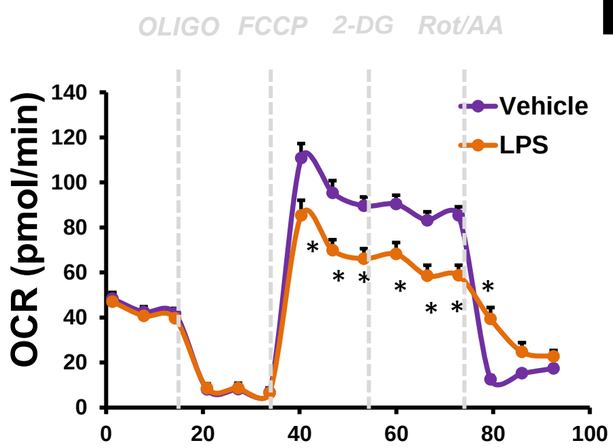

D

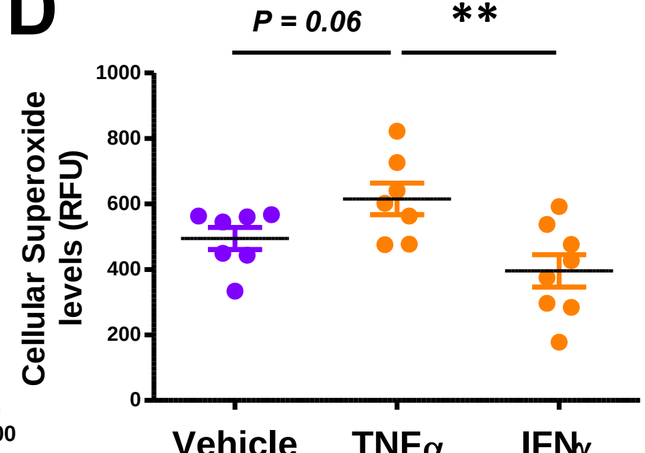

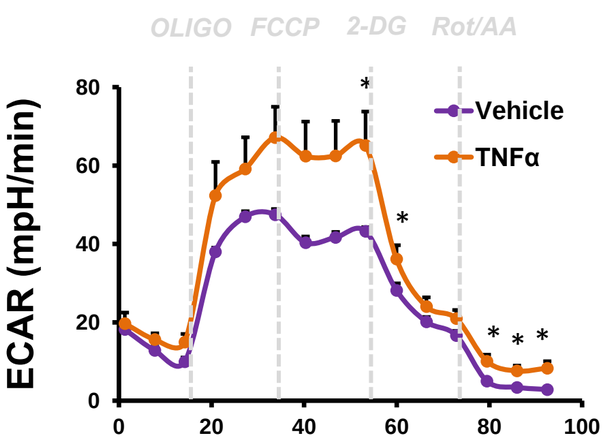

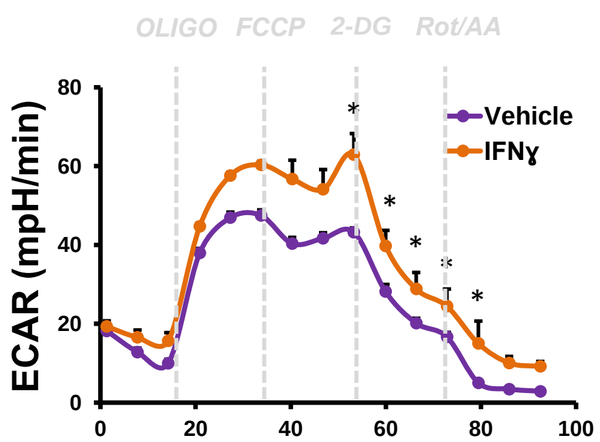

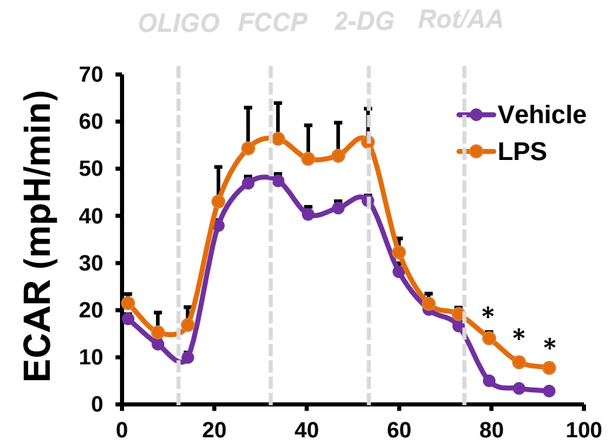

E

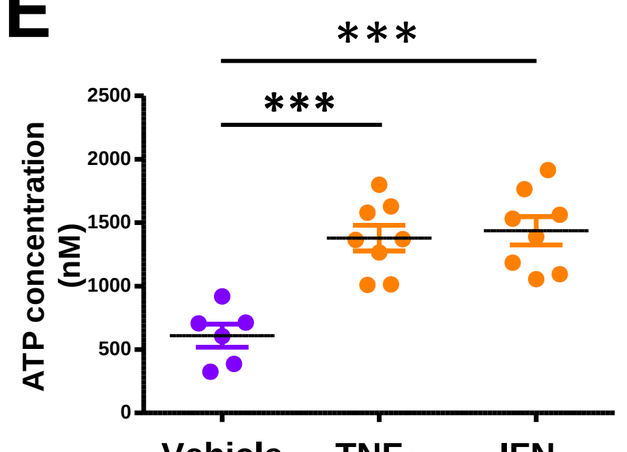

FIGURE LEGENDS – SUPPLEMENTAL

Figure S1. Study workflow. Simplified workflow, including laser-capture microdissection of glomerular and tubulointerstitial compartments, sample preparation followed by LC-MS/MS, data analysis by MaxQuant, statistical analysis to identify differentially expressed proteins (Perseus software), gene ontology (R 4.0.0) and pathway enrichment analysis (pathDip), downstream *in silico* analyses and verification/validation studies. AMR, antibody-mediated rejection; ACR, acute cellular rejection; ATN, acute tubular necrosis; LC-MS/MS, liquid chromatography followed by tandem mass spectrometry; IHC, immunohistochemistry; LFQ, label-free quantification.

Figure S2. Histograms depicting the distribution of the original and imputed protein intensity values in our study samples. Each histogram represents the distribution of the log2 transformed intensity values among the proteins quantified in each of the biopsy samples in the glomeruli (A, n=28) or tubulointerstitium (B, n=30). Blue bars represent the count of intensity values determined by mass spectrometry, whereas red bars represent the distribution of the imputed intensity values. Two of the glomerular fractions were excluded from further analyses due to poor protein recovery, which was reflected in a flat, non-normal distribution.

Figure S3. Representative light and electron microscopic images and injury scores of ultrastructural alterations in AMR, ACR and ATN cases. Representative light microscopy images of AMR, ACR and ATN cases (A, 20X). Representative electron microscopy images of a glomerular capillary loop in each study group (B, 8000X). Dot plots show foot process effacement score (C), glomerular basement membrane thickness (D), proportion of loops with evidence of subendothelial new basement membrane formation (relative to the total number of loops studied in two glomeruli per biopsy (E)), and scores (0-3) of glomerular (F) and peritubular (G) endothelial cell swelling (4 to 7 cases/group were studied). Semiquantitative score legend: 0 = none; 1 = mild (<25%); 2 = moderate (25-50%); 3 = severe (>50%). AMR, antibody-mediated rejection; ACR, acute cellular rejection; ATN, acute tubular necrosis; GBM, glomerular basement membrane.

Figure S4. Collagen chains quantified and differentially expressed in the glomerular compartment. Panel A shows a heatmap of all the collagen chains quantified in at least one kidney compartment. The mean protein expression values of the different chains of type IV collagen across the 3 studied groups (AMR, ACR, and ATN) in the glomeruli are represented by dot plots (B). *P<0.05. AMR, antibody-mediated rejection; ACR, acute cellular rejection; ATN, acute tubular necrosis; COL4, type IV collagen.

Figure S5. Distribution of the Q values of the pathways significantly enriched in the AMR glomeruli and tubulointerstitium. For each compartment, the significantly enriched pathways from Pathdip were classified using a reduction algorithm. Each dot represents the Q value (after Benjamini-Hochberg adjustment) of each particular pathway class. In both compartments, pathways enriched among proteins decreased in AMR and related to 'extracellular matrix and cell communication' showed a higher frequency of very low Q values (Q<0.005), as compared to the rest of the pathway classes, indicating a more significant enrichment. AMR, antibody-mediated rejection; ACR, acute cellular rejection; ATN, acute tubular necrosis; ECM, extracellular matrix.

Figure S6. Characterization of human glomerular microvascular endothelial cells. To confirm that HGMECs exhibited the expected endothelial cell phenotype at passage 5, the expression of endothelial cell-specific markers PECAM1, CHD5, and VWF in HGMECs, but not in other cell lines (namely human lung fibroblasts and renal proximal tubular epithelial cells (PTECs) was corroborated by real-time quantitative PCR and normalized to GAPDH. Lower expression of ACTA2 in HGMECs as compared to fibroblasts was also confirmed (A). HGMECs displayed the expected change in cell morphology towards a more oval, spindle-shaped phenotype in response to treatment with 1000U/mL IFNɣ or 10ng/mL TNFα for 24h (B). Magnification: 20x. Scale bar: 20µm. The phenotype changes after cytokine treatment were accompanied by a significant increase in CXCL10 and ACTA2 gene expression (C). Western blot and subsequent densitometry analysis showed that HGMECs expressed HLA class I but not HLA class II protein at baseline. Moreover, treatment with 500U/mL or 1000U/mL IFNɣ for 24h induced HLA II protein expression, and 1000U/mL IFNɣ increased HLA I protein expression, which was most accentuated 48 hrs after treatment (D). Both vehicle- and IFNɣ-pretreated HGMECs displayed the expected rapid increase in Erk phosphorylation upon stimulation with 1µg/mL α-HLA-I (E). Stimulation of HGMECs with 1µg/mL α-HLA-I, 1000U/mL IFNɣ or 10ng/mL TNFα for 24h elicited a proliferative response, as evidenced by increased intracellular RNA and DNA levels (F). To characterize the inflammatory response of HGMECs to α-HLA-I stimulation, cells were exposed to vehicle or 1µg/mL α-HLA-I for 24h, and secreted levels of IL-8, CCL2, and IL-4 were assessed in the cell supernatant by Multiplex ELISA (G). Gene expression levels of IL8, IL6, and VCAM1 (G) were also measured in HGMECs after exposure to vehicle, 5µg/mL of α-HLA-I, or 5µg/mL of isotype control for 12h, and normalized to VCL (H). Data are represented as mean ± SEM. *P<0.05; **P<0.01; ***P<0.001. HGMECs, human glomerular microvascular endothelial cells; PTECs, proximal tubular epithelial cells; ACTA2, aortic smooth muscle actin; PECAM1, platelet endothelial cell adhesion molecule; CHD5, cadherin-5; vWF, von Willebrand factor;

GAPDH, glyceraldehyde-3-phosphate dehydrogenase; CXCL10, C-X-C motif chemokine 10; MHC, major histocompatibility complex; IFNγ, interferon gamma; TNFα, tumor necrosis factor alpha; α-HLA-I, anti-HLA class I antibodies; ERK, mitogen-activated protein kinase; IL-4, interleukin-4; IL6, interleukin-6; CXCL8/IL-8, interleukin-8; CCL2, C-C motif chemokine 2; VCAM1, vascular cell adhesion protein 1; VCL, vinculin.

Figure S7. Characterization of regulated proteins and predicted proteases in the AMR glomeruli in human glomerular microvascular endothelial cells. Gene expression of TAP1 and HLA-C in HGMECs was upregulated by α-HLA-I and after stimulation with 1,000U/mL IFNγ for 24h (A). The effects of α-HLA-I and IFNγ on the gene expression of key proteases, namely CTSV, CTSL, CTSS, and MMP2, were also studied (B). Glycolysis (ECAR) and oxygen consumption rate (OCR) were monitored in a Seahorse XFe96 analyzer in HGMECs (C). The following concentrations were employed: oligomycin: 1µM; FCCP: 0.6µM, 2-DG: 100mM; Rot: 1mM; AA: 1mM. Oligomycin induces an increase in glycolysis by inhibiting ATP synthase. FCCP induces mitochondrial stress by uncoupling respiration from ATP synthesis. Rot/AA are electron transport chain inhibitors. *P<0.05 vs. Vehicle; #P<0.05 vs. isotype control-treated HGMECs. α-HLA-I stimulation in HGMECs increased levels of superoxide ion (D). Together with IFNγ and TNFα, α-HLA-I also induced an increase in the intracellular levels of ATP (E). Data are expressed as mean ± SEM. *P<0.05; **P<0.01; ***P<0.001. HGMECs, human glomerular microvascular endothelial cells; α-HLA-I, anti-HLA class I antibodies; IFNγ, interferon gamma; TNFα, tumor necrosis factor alpha**;** TAP1, antigen peptide transporter 1; HLA-C, HLA class I histocompatibility antigen, C alpha chain; CTSV, cathepsin-V; CTSL, cathepsin-L; CTSS, cathepsin-S; MMP2, matrix metalloproteinase-2; GAPDH, glyceraldehyde-3-phosphate dehydrogenase; RPL31, 60S ribosomal protein L31; ECAR, extracellular acidification rate; OCR, oxygen consumption rate; FCCP, p-trifluoromethoxy carbonyl cyanide phenyl hydrazone; 2-DG, 2-deoxyglucose; Rot, rotenone; AA: antimycin A.

Figure S8. Characterization of the inflammatory response of PTECs upon exposure to key cytokines in the AMR tubulointerstitium

PTECs displayed a modest change in cell morphology towards a more oval, spindle-shaped phenotype in response to treatment with 20ng/mL TNFα or 1ng/mL LPS for 24h. This change was more evident upon treatment with 1000U/mL IFNɣ for 24h (A). Magnification: 20x. Scale bar: 50µm. To relate morphological changes to the expected dysregulation of proinflammatory genes after cytokine treatment, the gene expression of IL6 (B), CCL2 (C), and CXCL10 (D) was determined and normalized to ACTB. Data are represented as mean ± SEM. *P<0.05; **P<0.01;

***P<0.001. PTECs, proximal tubular epithelial cells; IL6, interleukin-6; CCL2, C-C motif chemokine 2; CXCL10, C-X-C motif chemokine 10; ACTB, beta-actin; IFNγ, interferon gamma; TNFα, tumor necrosis factor alpha; LPS, lipopolysaccharide.

Figure S9. Characterization of regulated proteins and predicted proteases in the AMR tubulointerstitium in primary human proximal tubular epithelial cells

Protein expression of GSTO1 was analyzed in PTECs after treatment with vehicle, 20ng/µL of TNFα, 1000U/mL of IFNγ, or 1ng/µL of LPS for 24h, and normalized to GAPDH (A). The immunoblots and corresponding densitometry values are shown. GSTO1 expression was also measured at the gene level after treatment with vehicle, 20ng/µL of TNFα, or 1000U/mL of IFNγ for 24h (A). The effects of TNFα and IFNγ on the gene expression of CTSL, CTSV, CTSS, and LGMN proteases, were studied (B). OCR and ECAR were monitored in a Seahorse XFe96 analyzer in order to study the effects of TNFα, IFNγ, or LPS on PTECs. As expected, LPS-treated PTECs (positive control) experienced a metabolic switch towards a more glycolytic phenotype, compared to vehicle-treated cells (C). The following concentrations were employed: oligomycin: 1µM; FCCP: 0.3µM, 2-DG: 100mM; Rot: 1mM; AA: 1mM. Oligomycin induces an increase in glycolysis by inhibiting ATP synthase. FCCP induces mitochondrial stress by uncoupling respiration from ATP synthesis. Rot/AA are electron transport chain inhibitors. *P<0.05 vs. Vehicle-treated PTECs. Intracellular levels of superoxide ion (D) and ATP (E) were also measured in vehicle-, TNFα-, and IFNγ-treated PTECs. Data are expressed as mean ± SEM. *P<0.05; **P<0.01; ***P<0.001. PTECs, human proximal tubular epithelial cells; TNFα, tumor necrosis factor alpha**;** IFNγ, interferon gamma; LPS, lipopolysaccharide; GSTO1, glutathione S-transferase omega-1; GAPDH, glyceraldehyde-3-phosphate dehydrogenase; CTSL, cathepsin-L; CTSV, cathepsin-V; CTSS, cathepsin-S; LGMN, legumain; ACTB, beta-actin; ECAR, extracellular acidification rate; OCR, oxygen consumption rate; FCCP, p-trifluoromethoxy carbonyl cyanide phenyl hydrazone; 2-DG, 2-deoxyglucose; Rot, rotenone; AA: antimycin A.